Computational Materials Science 71 (2013) 97–100

Contents lists available at SciVerse ScienceDirect

Computational Materials Science

journal homepage: www.elsevier.com/locate/commatsci

A Bayesian approach to 2D triple junction modeling

Basil Singer [a], Stephen Hyatt [b,*], Steve Drekic [a]

[a] Dept. of Statistics & Actuarial Science, University of Waterloo, Waterloo, Ontario, Canada
[b] School of Engineering, Northwestern Polytechnic University, Fremont, CA, USA

ARTICLE INFO

Article history:
Received 23 September 2012
Received in revised form 3 December 2012
Accepted 7 January 2013
Available online 16 February 2013

Keywords:
Coincident Site Lattice (CSL)
Crystallographic constraint
Special coordination
Grain boundary
Triple junction

ABSTRACT

We propose a Bayesian analytical approach to evaluate the 2D local transition probabilities model developed by Frary and Schuh in 2004 [1]. Their model characterizes the statistical properties of high-angle and low-angle interface networks in polycrystalline ensembles. The motivation for this work is to analyze the approach presented in Ref. [1] under a Bayesian premise. The model of Frary and Schuh [1] considers the percolation angular threshold for interfacial networks, Θ_t, to be a deterministic quantity; we, on the other hand, relax this assumption and presume the threshold angle to be a random variable. The physical justification for this is that there could be uncertainties in the microstructure network or measurement errors, for example, and thus Θ_t should not be a constant value. As a result, the fraction of boundaries to be classified as special, P, also becomes a random variable. We assume P to follow a Beta$(z, 1-z)$ distribution, where $z \in (0,1)$ is an adjustable parameter. Comparison of the error analysis between the Bayesian and non-Bayesian approaches, to the experimental results reported by Frary and Schuh [1], suggests that our model accounts for slightly more variation than the non-Bayesian approach.

1. Introduction

Frary and Schuh [1] and Minich et al. [2] identified the crystallographic constraint as a limiting factor that governs the extent of the probabilistic coordination of special character grain boundaries at triple junctions. The distinction between special and general grain boundaries is that the former is a Coincident Site Lattice (CSL) or low-angle boundary, while the latter is a non-CSL or high-angle boundary. Analysis of experimental data has shown that the special coordination of the grain boundaries are non-random [1,2]. These non-random coordinations are attributed to the underlying crystallographic constraints required to maintain consistency and connectivity of grain orientations around triple junctions. This was validated through global grain boundary modeling [1,2], and it was found that boundaries of the same type tend to cluster (i.e., high-angle with high-angle, low-angle with low-angle) [1].

The comparison of 2D global grain boundary models with experimental results led to the identification of percolation thresholds for the different crystal classes and grain disorientation constraints [1]. Frary and Schuh used these constraints to derive and calculate the local transition probabilities around a triple junction. In what follows, we adopt the notation used by Frary and Schuh [1]: let ϕ express the grain rotation subject to a maximum rotation, and θ_t, a threshold-parameter, to distinguish special boundaries from general ones. The parameter ϕ is the orientation tolerance of the grains that controls the range of grain boundary misorientation angles, θ, in the grain boundary network. The parameters $\phi_{\max}$ and $\theta_{\max}$ are, respectively, the grain rotation limit and the maximum disorientation of the three boundaries at the triple junction. When ϕ is large, the microstructures approach a perfect random texture; conversely, as ϕ decreases, the microstructures approach a perfect fiber texture.

The crystallographic constraint around the triple junction, namely the circuital grains A, B, and C that share a common axis, is quantitatively expressed by the deviation limit constraint rule. For instance, letting θ_A and θ_B be the grain boundaries opposite grains A and B, respectively, and θ_C be the disorientation of the grain boundary at the triple junction, the inequality $\theta_C \leqslant \theta_A + \theta_B$ must be satisfied.

Another feature of the crystallographic constraint is that the grain boundary disorientations may be determined as the difference between the orientations of the neighboring grains (e.g., $\theta_C = \phi_A - \phi_B$) and may take any value on the range $(-2\phi_{\max}, 2\phi_{\max})$. In addition, the grain boundary disorientations around a circuit of the triple junction are defined by the expression $\theta_A + \theta_B + \theta_C = 0$, and are similarly constrained when rotated about a single axis.

By defining local transition probabilities and incorporating the above-mentioned crystallographic constraints, Frary and Schuh [1] obtained expressions for the "local fraction of triple junctions

* Corresponding author. Fax: +1 510 657 8975.
E-mail addresses: bksinger@uwaterloo.ca (B. Singer), stephenhyatt@mail.npu.edu (S. Hyatt), sdrekic@uwaterloo.ca (S. Drekic).

0927-0256/$ - see front matter © 2013 Elsevier B.V. All rights reserved.
http://dx.doi.org/10.1016/j.commatsci.2013.01.012

coordinated by i special boundaries" for $i = 0$, 1, 2, and 3 under a non-Bayesian setting. In particular, they derived the following formula for p, the global low-angle fraction:

$$p = \frac{\theta_t}{\phi_{\max}} - \left(\frac{\theta_t}{2\phi_{\max}}\right)^2. \tag{1}$$

Based on the values that the parameters $\phi_{\max}$ and θ_t can assume, we remark that $p \in (0,1)$.

2. Analytical model

2.1. The transition probabilities of the non-Bayesian model

Using Frary and Schuh's notation [1], let J_i represent the fraction of "triple junctions coordinated by i special boundaries" for $i = 0$, 1, 2, and 3. When the deviation limit constraint rule is satisfied, the expressions for the J_i's are based on products of local transition probabilities. Specifically, letting Π_x^y denote the local density distribution of low-angle boundaries at a triple junction where y is the number of boundaries that have been assigned ($y = 0$, 1 or 2) and x is the number of boundaries that have been classified as special ($x \leqslant y$), Frary and Schuh [1] obtained the following results:

$$J_0 = (1-\Pi_0^0)(1-\Pi_0^1)(1-\Pi_0^2), \tag{2a}$$

$$J_1 = \Pi_0^0(1-\Pi_1^1)(1-\Pi_1^2) + (1-\Pi_0^0)\Pi_0^1(1-\Pi_1^2) + (1-\Pi_0^0)(1-\Pi_0^1)\Pi_0^2, \tag{2b}$$

$$J_2 = \Pi_0^0\Pi_1^1(1-\Pi_2^2) + \Pi_0^0(1-\Pi_1^1)\Pi_1^2 + (1-\Pi_0^0)\Pi_0^1\Pi_1^2, \tag{2c}$$

$$J_3 = \Pi_0^0\Pi_1^1\Pi_2^2. \tag{2d}$$

In the case of randomly coordinated boundaries at the triple junction, which we refer to as the random lattice case, all the local transition probabilities are equal to the same value. Specifically, Π_x^y is equal to p (which itself is given by Eq. (1)), and therefore Eqs. (2a)–(2d) simplify to yield a binomial distribution given by the well-known formula

$$J_i = \binom{3}{i} p^i (1-p)^{3-i}, \quad \text{for } i = 0,1,2,3.$$

In Frary and Schuh's model [1], the local transition probabilities are as follows:

$$\Pi_0^0 = p, \tag{3a}$$

$$\Pi_0^1 = \begin{cases} \frac{1-6(1-p)^{1/2}+15(1-p)-10(1-p)^{3/2}}{3(1-p)} & \text{for } p \leqslant 0.75 \\ \frac{3-2(1-p)^{1/2}}{3} & \text{for } p > 0.75 \end{cases}, \tag{3b}$$

$$\Pi_1^1 = \begin{cases} \frac{2+8(1-p)^{1/2}-10(1-p)}{3+3(1-p)^{1/2}} & \text{for } p \leqslant 0.75 \\ \frac{3-6(1-p)+2(1-p)^{3/2}}{3-3(1-p)} & \text{for } p > 0.75 \end{cases}, \tag{3c}$$

$$\Pi_0^2 = \begin{cases} \frac{2-12(1-p)^{1/2}+24(1-p)-14(1-p)^{3/2}}{-1+6(1-p)^{1/2}-12(1-p)+10(1-p)^{3/2}} & \text{for } p \leqslant 0.75 \\ 1 & \text{for } p > 0.75 \end{cases}, \tag{3d}$$

$$\Pi_1^2 = \begin{cases} \frac{1-5(1-p)^{1/2}+4(1-p)}{-1+5(1-p)^{1/2}-10(1-p)} & \text{for } p \leqslant 0.75 \\ \frac{3-4(1-p)^{1/2}}{3-2(1-p)^{1/2}} & \text{for } p > 0.75 \end{cases}, \tag{3e}$$

$$\Pi_2^2 = \begin{cases} \frac{3+6(1-p)^{1/2}}{2+10(1-p)^{1/2}} & \text{for } p \leqslant 0.75 \\ \frac{3-9(1-p)+6(1-p)^{3/2}}{3-6(1-p)+2(1-p)^{3/2}} & \text{for } p > 0.75 \end{cases}. \tag{3f}$$

2.2. The transition probabilities of the Bayesian model

2.2.1. Introducing a prior distribution

To distinguish between variables which are fixed (i.e., deterministic) and ones which are random, we define Θ_t and P to be the random counterparts of θ_t and p, respectively. In order to extend the results of Frary and Schuh [1] under a Bayesian framework, we assume Θ_t to be a random variable. However, the variables $\theta_{\max}$ and $\phi_{\max}$ are still assumed to be constant.

Maintaining the premise that the deviation limit constraint rule remains in effect, Eq. (1), as a result, will still hold. Therefore, P is a random variable, which we assume to have cumulative distribution function, $G(\cdot)$, on the interval $(0,1)$ with an expected value of $E[P] = z \in (0,1)$. This distribution is known as the prior distribution with z serving as the parameter of the underlying Bayesian model.

2.2.2. Redefining the transition probabilities

For notational convenience, we let $\Pi_x^y(p)$ denote the transition probabilities conditional on knowing that $P = p$. Therefore, in order to calculate Π_x^y, we need to integrate $\Pi_x^y(p)$ with respect to G in order to remove the dependence on p. In other words,

$$\Pi_x^y = \int_0^1 \Pi_x^y(p)\,dG(p). \tag{4}$$

Note that for the random lattice case introduced earlier, P is a deterministic quantity (i.e., $G(p) = 0$ for $p < z$ and $G(p) = 1$ for $p \geqslant z$) and this implies that it will always be equal to its expected value, namely z. Hence, it immediately follows that $\Pi_x^y = \Pi_x^y(z) = z$.

In Frary and Schuh's model [1], since Θ_t is assumed to be a fixed quantity, P is also fixed and so it too will always be equal to its expected value. Hence, $\Pi_x^y = \Pi_x^y(z)$ where $\Pi_x^y(z)$ is given by Eqs. (3a)–(3f) with p replaced by z.

2.2.3. The Beta distribution model

In contrast to the previous two models in which P was a deterministic quantity, let us now assume that the random variable P follows a Beta$(z, 1-z)$ distribution [3] where $z \in (0,1)$. The beta distribution provides a simple and flexible probability distribution to model the random variable P, having associated probability density function $g(p) = G'(p)$ given by

$$g(p) = \begin{cases} \frac{1}{B(z,1-z)} p^{z-1}(1-p)^{-z} & \text{for } p \in (0,1) \\ 0 & \text{otherwise} \end{cases}, \tag{5}$$

where $B(z, 1-z) = \int_0^1 w^{z-1}(1-w)^{-z}dw$ denotes the so-called beta function and $E[P] = z$. Under Eq. (5), we immediately note that Eq. (4) becomes

$$\Pi_x^y = \int_0^1 \Pi_x^y(p)g(p)dp. \tag{6}$$

For the random lattice case, recall again that $\Pi_x^y(p) = p$. Therefore, Eq. (6) simplifies to give $\Pi_x^y = \int_0^1 pg(p)dp = E[P] = z$, which is identical to the result obtained in the non-Bayesian case. On the other hand, however, it is evident that substituting Eqs. (3a)–(3f) into Eq. (6) will yield different results than those obtained by Frary and Schuh [1] in their non-Bayesian model. In what follows, we refer to this particular variant as "Frary and Schuh's Bayesian model".

2.2.4. Numerical results

Figs. 1–4 provide graphical comparisons of the J_i's (viewed as a function of $z \in (0,1)$) between (a) Frary and Schuh's Bayesian model (solid lines), (b) Frary and Schuh's non-Bayesian model (dotted lines), and (c) the random lattice case (dashed lines). Experimental results (denoted by diamonds in these figures) were reproduced from Ref. [1]. We further remark that in the case of Frary and Schuh's

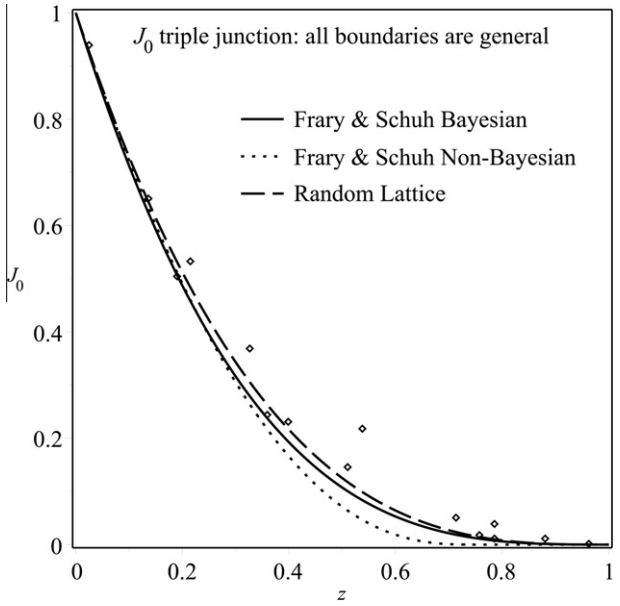

Fig. 1. Triple junction distribution comparison between Frary and Schuh's Bayesian model, Frary and Schuh's non-Bayesian model, and the random lattice case for J_0.

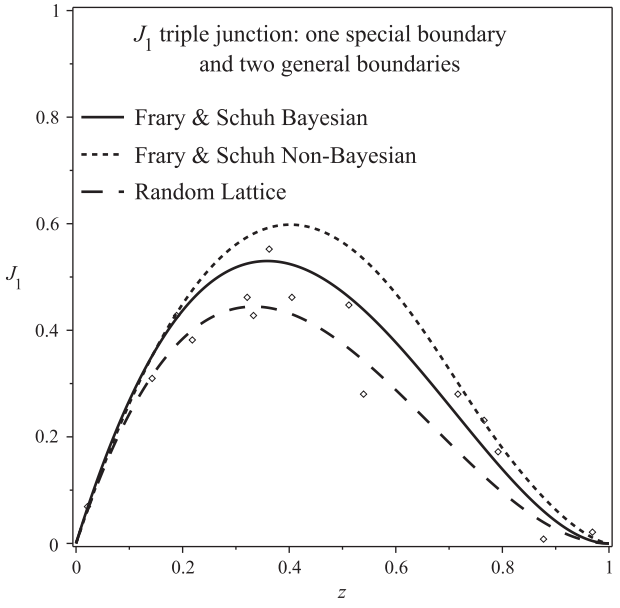

Fig. 2. Triple junction distribution comparison between Frary and Schuh's Bayesian model, Frary and Schuh's non-Bayesian model, and the random lattice case for J_1.

Bayesian model, the integration step in Eq. (6) was performed numerically using the mathematical software package *Maple 16*.

In looking at the figures, we observe that Frary and Schuh's Bayesian model yields in all cases (except for J_2, although the results are very close) more accurate results than its non-Bayesian counterpart when compared to the results obtained experimentally. For instance, experimental results for $z < 0.75$ in Fig. 2 appear to be much closer to the Bayesian model (solid line) and the random lattice case (dashed line) for J_1 coordination. In the way of further evidence, Table 1 displays the sum of squared errors when comparing the Bayesian and non-Bayesian approaches (as well as the random lattice case) to the experimental data (which was digitized for these plots from Ref. [1]). Table 1 suggests that the Bayesian model provides the best overall performance over the entire set of coordinations.

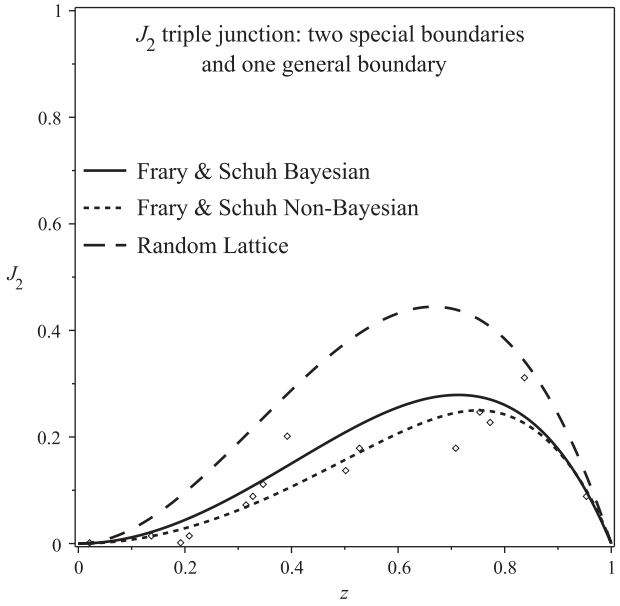

Fig. 3. Triple junction distribution comparison between Frary and Schuh's Bayesian model, Frary and Schuh's non-Bayesian model, and the random lattice case for J_2.

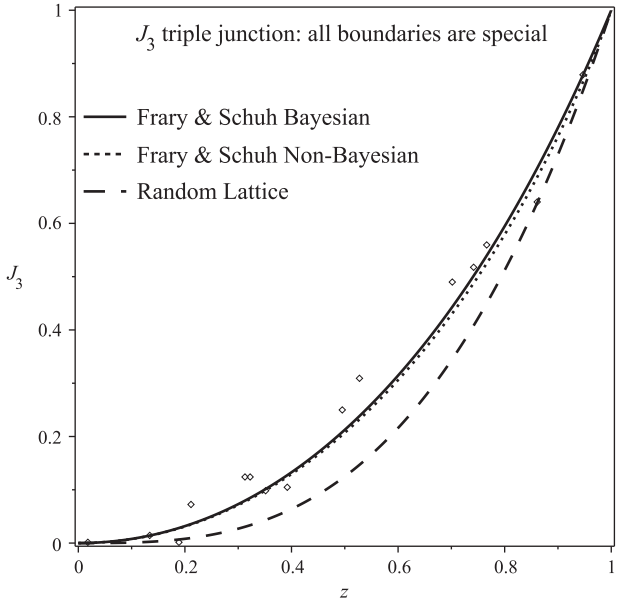

Fig. 4. Triple junction distribution comparison between Frary and Schuh's Bayesian model, Frary and Schuh's non-Bayesian model, and the random lattice case for J_3.

Table 1
Error analysis comparing results of models to experimental data. The values below were calculated following the sum of squared errors (SSEs) method (i.e., $\text{SSE} = \Sigma(x_{\text{model},z} - x_{\text{experiment},z})^2$).

J_i	Frary and Schuh's Bayesian model vs. experimental data	Frary and Schuh's non-Bayesian model vs. experimental data	Random lattice case vs. experimental data
J_0	0.04	0.06	0.02
J_1	0.06	0.15	0.06
J_2	0.03	0.02	0.32
J_3	0.02	0.02	0.11

3. Conclusion and future research

We have shown that by incorporating a Bayesian premise on Frary and Schuh's model [1], the resulting model yields closer results to the experimental data than their originally proposed model. The results, however, are slight, so it would be desirable to explore other probability distributions for P that could yield even closer results to the experimental data. Moreover, it might also be worth investigating candidate distributions for Θ_t as a means of establishing a framework for characterizing the fraction of boundaries to be classified as special, so as to provide the best possible fit to the experimental data.

Acknowledgements

The authors would like to thank the referee for his/her useful remarks and suggestions which helped improve an earlier version of this paper. The authors also gratefully acknowledge the feedback and opinions of Dr. M. Frary.

References

[1] M. Frary, C.A. Schuh, Phys. Rev. B 69 (2004) 134115-1–134115-12.
[2] R.W. Minich, C.A. Schuh, M. Kumar, Phys. Rev. B 66 (2002) 052101-1–052101-4.
[3] N.A. Weiss, A Course in Probability, Pearson Addison Wesley, Boston, 2006.